Understanding the Change in Streamflow of an Inland River as a Response to Regional Climate Change in Northwest China

Yiwen Xu[1,2], Jianhua Xu[1,2]*
[1]College of Resources and Environmental Science, East China Normal University, Shanghai, China
[2]Research Center for East-West Cooperation in China, East China Normal University, Shanghai, China
*Corresponding author, e-mail: jhxu@geo.ecnu.edu.cn

Abstract—**The hydro-climatic process in arid areas is an important academic issue, which has been paid more and more attentions since the 1990s. But to date, it has not received satisfactory answers. From a perspective of multi-time scales, this paper studied the relationship between the stream flow of an inland river and its related climatic factors in the arid area of northwest China by an integrated approach combining wavelet decomposition (WD), multiple linear regression (MLR), and back propagation artificial neural network (BPANN), and investigated the Yarkand River in the southern Xinjiang as a case study. The results show that the annual runoff (AR) was mainly affected by the annual average temperature (AAT) and annual precipitation (AP), which revealed different variation patterns at five time scales. At the 16- year and 32- year scale, AR basically presented a monotonically increasing trend with the similar trend of AAT and AP. But at 2-year, 4-year, 8-year and 16-year scale, AR presented nonlinear variation with fluctuations of AAT and AP.**

Keywords-streamflow; inland river; climate change; Xinjiang, northwest China

I. INTRODUCTION

Theoretically, a hydro-climatic process can be evaluated to determine if it is in an ordered, deterministic system; an unordered, random system; or a chaotic, dynamic system, and whether change patterns of periodicity or quasi-periodicity exist. However, it is difficult to achieve a thorough understanding of the complex mechanism of a hydro-climatic process [1]. Specifically, there still lack effective means to thoroughly discover the dynamics of hydro-climatic processes at different time scales [2]. Therefore, more studies are required to explore the hydro-climatic process from different perspectives and using different methods [3, 4]. Specific to the Yarkand River, a question of interest will be the variation patterns of the hydro-climatic process at different time scales. To date, this question has not been answered satisfactorily [5].

The inland rivers of northwest China (NW China), such as the Yarkand River, which has been relatively undisturbed by human activities, is mainly recharged by snowmelt. The main climate factors directly affecting the recharge of the river are temperature and precipitation. Due to the complexity of the hydro-climatic system, it is difficult to understand the mechanism of hydro-climatic process thoroughly [6, 7].

Using an integrated approach combining wavelet decomposition (WD), multiple linear regression (MLR), and back propagation artificial neural network (BPANN), this paper studied the relationship between the streamflow of inland river and its related climatic factors at different time scales, and then analyzed the simulated results in the Yarkand River of southern Xinjiang as an example.

II. METHODOLOGY

A. General idea

In order to reveal the streamflow of inland river and its response to regional climate change at different time scales, this paper conducted an integrated approach combining wavelet decomposition (WD), multiple linear regression (MLR), and back propagation artificial neural network (BPANN). Firstly, the WD was used to reveal the variation patterns of streamflow and its related climatic factors at different time scales. Then, the relationship between streamflow and its related climatic factors was simulated by BPANN and MLR based on WD at different time scales.

B. Wavelet decomposition (WD)

Wavelet transformation has been shown to be a powerful technique for characterizing the frequency, intensity, time position, and duration of variations in climate and hydrological time series [8, 9, 22]. Wavelet analysis can also reveal localized time and frequency information without requiring the time series to be stationary, as required by the Fourier transform and other spectral methods [10].

A continuous wavelet function $\Psi(\eta)$ that depends on a nondimensional time parameter η can be written as (Labat, 2005):

$$\Psi(\eta) = \Psi(a,b) = |a|^{-1/2}\ \Psi(\frac{t-b}{a}) \qquad (1)$$

where, t denotes time, a is the scale parameter and b is the translation parameter. $\Psi(\eta)$ must have a zero mean and be localized in both time and Fourier space. The continuous wavelet transform (CWT) of a discrete signal, x(t), such as the time series of runoff, temperature, or precipitation, is expressed by the convolution of x(t) with a scaled and translated $\Psi(\eta)$,

$$W_x(a,b) = |a|^{-1/2} \int_{-\infty}^{+\infty} x(t)\Psi^*(\frac{t-b}{a})dt \quad (2)$$

where, * indicates the complex conjugate, and $W_x(a, b)$ denotes the wavelet coefficient. Thus, the concept of frequency is replaced by that of scale, which characterizes the variation in the signal, x(t), at a given time scale.

Selecting a proper wavelet function is a prerequisite for time series analysis. The actual criteria for wavelet selection include self-similarity, compactness, and smoothness. For the present study, Symlet 8 was chosen as the wavelet function according to these criteria.

The nonlinear trend of a time series, x(t), can be analyzed at multiple scales through wavelet decomposition on the basis of the discrete wavelet transform (DWT). The DWT is defined taking discrete values of a and b. The full DWT for signal, x(t), can be represented as [11]:

$$x(t) = \sum_k \mu_{j_0,k}\phi_{j_0,k}(t) + \sum_{j=1}^{j_0}\sum_k \omega_{j,k}\psi_{j,k}(t) \quad (3)$$

where $\phi_{j_0,k}(t)$ and $\psi_{j,k}(t)$ are the flexing and parallel shift of the basic scaling function, $\phi(t)$, and the mother wavelet function, $\psi(t)$, and $\mu_{j_0,k}(j < j_0)$ and $\omega_{j,k}$ are the scaling coefficients and the wavelet coefficients, respectively. Generally, scales are based on powers of 2, which is the dyadic DWT.

Once a mother wavelet is selected, the wavelet transform can be used to decompose a signal according to scale, allowing separation of the fine-scale behavior (detail) from the large-scale behavior (approximation) of the signal [12]. The relationship between scale and signal behavior is designated as follows: a low scale corresponds to compressed wavelet as well as rapidly changing details, namely high frequency, whereas a high scale corresponds to stretched wavelet and slowly changing coarse features, namely low frequency. Signal decomposition is typically conducted in an iterative fashion using a series of scales such as a = 2, 4, 8, ..., 2^L, with successive approximations being split in turn so that one signal is broken down into many lower resolution components.

The wavelet decomposition (WD) and reconstruction were used to approximate the nonlinear variation of streamflow and its related climatic factors over the entire study period at the selected different time scales.

C. *BPANN based on wavelet decomposition*

In order to disclose the relationship between streamflow with its related climatic factors at different time scales, this study employed the back propagation artificial neural network (BPANN) based on the results of wavelet decomposition. We first approximated the variation patterns of runoff and its related climate factors, such as AR, ATT and AP using wavelet decomposition on the basis of the discrete wavelet transform (DWT) at different time scales. Then the relationship between AR with AAT and AP were revealed by using BPANN based on the wavelet approximation [21].

In back-propagation networks, a number of smaller processing elements (PEs) are arranged in layers: an input layer, one or more hidden layers, and an output layer [13, 18]. The input from each PE in the previous layer (x_i) is multiplied by a connection weight (w_{ji}). These connection weights are adjustable and may be likened to the coefficients in statistical models. At each PE, the weighted input signals are summed and a threshold value (θ_j) is added. This combined input (I_j) is then passed through a non-linear transfer function ($f(\cdot)$) to produce the output of the PE (y_j). The output of one PE provides the input to the PEs in the next layer. This process can be summarized in equations as follows [14]:

$$I_j = \sum w_{ji}x_i + \theta_j \quad (4)$$

$$y_i = f(I_j) \quad (5)$$

Our ANN model is a three-tier structure: an input X with two variables (i.e. AAT and AP) is linearly mapped to intermediate variables (called hidden neurons) H, which are then nonlinearly mapped to the output y (i.e. AR).

By comparing the advantages and disadvantages of artificial neural network transfer functions, we selected the activation function as the hyperbolic tangent sigmoid transfer function, and Levenberg-Marquardt (trainlm) as the training function.

The purpose of the model is to capture the relationship between a historical set of model inputs and corresponding outputs. As mentioned above, this is achieved by repeatedly presenting examples of the input/output relationship to the model and adjusting the model coefficients (i.e. the connection weights) in an attempt to minimize an error function between the historical outputs and the outputs predicted by the model. This calibration process is generally referred to as 'training'. The aim of the training procedure is to adjust the connection weights until the global minimum in the error surface has been reached.

The back-propagation process is commenced by presenting the first example of the desired relationship to the network. The input signal flows through the network, producing an output signal, which is a function of the values of the connection weights, the transfer function and the network geometry. The output signal produced is then compared with the desired (historical) output signal with the aid of an error (cost) function.

D. *Wavelet regression analysis*

To compare the simulated results from BPANN with those from multiple linear regression (MLR) at different time scales, we also employed the wavelet regression analysis, i.e. regression based on WA. This method fits multiple linear regression equation (MLRE) between AR with AAT and AP by using multiple linear regression (MLR) based on the results of wavelet approximation [3, 4, 19].

The multiple linear regression model is

$$y = a_0 + a_1x_1 + a_2x_2 + ... + a_kx_k \quad (6)$$

where, y is dependent variable, x_i the independent variables; a_i is the regression coefficient, which is generally calculated by method of least squares [15]. In this study, the dependent variable is the annual runoff (AR) and the independent variables are related climatic factors, such as the annual average temperature (AAT) and annual precipitation (AP), etc.

E. Model test

In order to identify the uncertainty of the estimates for a given timescale, the coefficient of determination was calculated as follows:

$$\mathrm{CD} = 1 - \frac{RSS}{TSS} = 1 - \frac{\sum_{i=1}^{n}(y_i - \hat{y}_i)^2}{\sum_{i=1}^{n}(y_i - \bar{y})^2} \quad (7)$$

where CD is the coefficient of determination; $\hat{y}_i$ and y_i are the simulate value and actual data of runoff respectively; $\bar{y}$ is the mean of $y_i (i = 1,2,...,n)$; $RSS = \sum_{i=1}^{n}(y_i - \hat{y}_i)^2$ is the residual sum of squares; $TSS = \sum_{i=1}^{n}(y_i - \bar{y})^2$ is the total sum of squares. The coefficient of determination is a measure of how well the simulate results represent the actual data. A bigger coefficient of determination indicates a higher certainty and lower uncertainty of the estimates [15].

To compare the relative goodness between the ANN and multiple linear regression (MLR) fit for a given timescale, we also used the measure of Akaike information criterion (AIC) [16]. The formula of AIC is as follows:

$$AIC = 2k + n\ln(RSS/n) \quad (8)$$

where k is the number of parameters estimated in the model; n is the number of samples; RSS is the same as in formula (7). A smaller AIC indicates a better model.

For small sample sizes (i.e., n/K≤40), the second-order Akaike Information Criterion (AICc) should be used instead

$$AIC_c = AIC + \frac{2k(k+1)}{n-k-1} \quad (9)$$

where n is the sample size. As the sample size increases, the last term of the AICc approaches zero, and the AICc tends to yield the same conclusions as the AIC [16].

III. A CASE STUDY OF YARKAND RIVER, SOUTHERN XINJIANG, NW CHINA

A. Study Area and data

The Yarkand River (Figure.1) is located in the southeastern of Xinjiang Uygur Autonomous Region, northwest China (NW China), with a length of 1097km. The Yarkand River Basin (35°40′ ~ 40°31′N, 74°28′ ~ 80°54′E) has a total area of 9.89×10^4km^2, including 6.08×10^4km^2 as the mountain area, which accounts for 61.5%, and 3.81×10^4km^2 as the plain area, which takes up 38.5% [20]. The main stream of Yarkand River originates from Karakoram Pass in the north slope of the Karakoram Mountain, which is full of towering peaks and developmental glaciers, as well as the extremely rare precipitation on the plains. Due to the special geographical conditions, the accumulation of ice and snow in high mountains is the only supply for runoff. Therefore, the Yarkand River is a typical ice and snow supply river, in which the multi-year average runoff in the Kaqun hydrometric station consists of 64.0% from mean volume of glacial ablation, 13.4% from rain and snow supply, and 22.6% from groundwater supply, respectively [8].

The Yarkand River is an inland river, with no water recharge in the plain area; its stream flow mainly comes from mountainous area, i.e., the Pamir Mountains. In other words, the runoff of the Yarkand River is in turn mainly fed by glacier, snowmelt and precipitation in the Pamir Mountains. Therefore, the climatic factors, especially temperature and precipitation, directly affect the annual changes in the runoff. So we use the runoff as well as temperature and precipitation data to analyze the nonlinearity of the annual runoff process in the Yarkand River. The runoff data were from the Kaqun hydrologic station, and temperature and precipitation data were from Tash Kurghan meteorological station. The two stations are located in the source areas of the river and the amount of water used by humans is minimal compared to the total discharge. Therefore, it was assumed that the observed hydrological and meteorological records reflect the natural conditions.

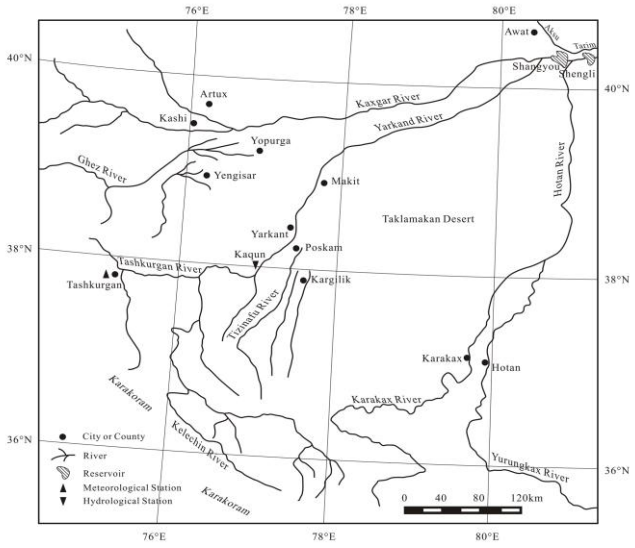

Figure 1. Location of the Study Area

Long-term climate changes can alter the runoff production pattern, the timing of hydrological events, and the frequency and severity of floods, particularly in arid or semi-arid regions. Therefore, a small change in precipitation and temperature may result in marked changes in runoff. To investigate the runoff and its related climatic effect, this study used the time series data of annual runoff (AR), annual average temperature (AAT) and annual precipitation (AP) from 1957 to 2008.

B. Climate factors affecting streamflow

Our previous study indicated that [18], the annual average temperature and annual precipitation are the most important

factors that are related with the annual runoff. The result was also supported by the other studies for the headwaters of the Tarim River Basin [17].

The raw data of the annual runoff (AR), annual average temperature (AAT) and annual precipitation (AP) showed in fluctuating patterns (Figure 2). However, it is difficult to identify any trends or periodicity simply based on the surface of the oscillation pattern. In order to reveal the trends of AR, AAT and AP at different time scales, the above wavelet analysis method was used.

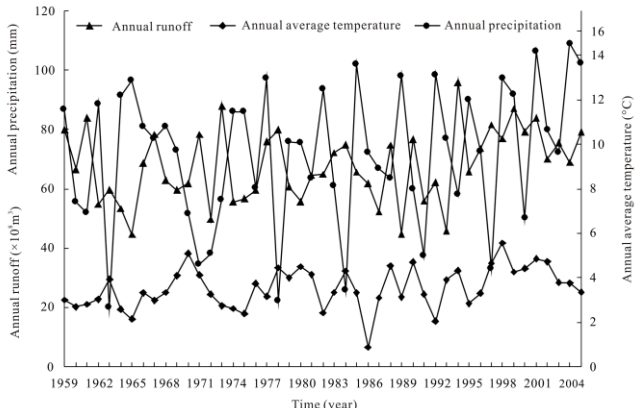

Figure 2. The Raw Data of AR, AAT and AP

The wavelet decomposition (WD) for the time series of annual average temperature (AAT) at different time scales is shown in Figure 3.

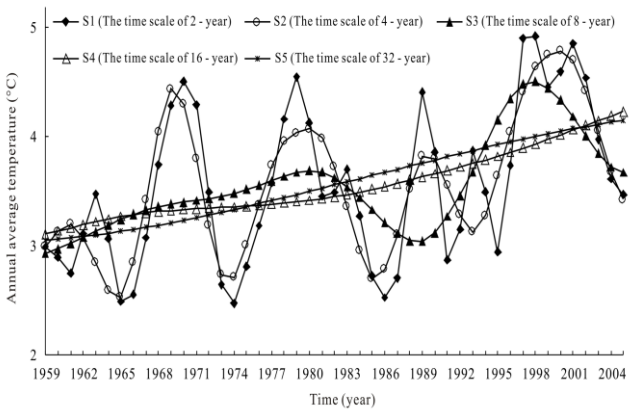

Figure 3. The variation patterns of AAT at different time scales

Figure 3 showed five variation patterns of AAT at five time scales. The five time scales are designated as S1 to S5, which represent 2- year, 4-year, 8-year, 16-year and 32-year time scale respectively. There are drastic fluctuations in the curve S1 and S2. The curve S3 is getting smoother and the increasing trend becomes even more obvious as the scale level increases. The curve S4 and S5 basically show a monotonic increasing trend.

Accordingly, the wavelet decomposition for the time series of AP and AR resulted in five variation patterns at five time scales.

The results tell us that variation patterns of all AR, AAT and AP were dependent on the time scales.

C. Relationship between streamflow and climatic factors

For the purpose of understanding the relationship between the AR and AAT & AP, based on the results of WD at five time scales, the back-propagation artificial neural network (BPANN) was employed.

Our study considered a three-layer BPANN, i.e. input layer, output layer and hidden layer, to simulate the nonlinear relationship between AR with AAT, and AP at each time scale. The input layer contains two variables, i.e. AAT and AP, the output layer contains one variable i.e. AR, and the neuron number of hidden layer is different with BPANN on different time scales, and it is 3, 5, 5, 5 and 4 respectively. TABLE 1 shows the optimized parameters for BPANN at different time scales.

The numerical work was carried out using MATLAB. We selected tansig as the transfer function, and trainlm as the training function to train network.

Based on wavelet decomposition results of AR, AAT and AP from 1957 to 2008, we randomly extracted 80%, 10% and 10% of the data as training, validation and testing samples, respectively. The results show that, at the time scales of S1, S2, S3, S4 and S5 (i.e. 2-year, 4-year 8-year, 16-year, and 32-year), all network models have reached the expected error target (0.001) with learning rate of 0.01. The optimized parameters of the BPANN for the hydro-climatic process at different time scales are shown in TABLE I.

TABLE I. BASIC PARAMETERS OF THE BPANN AT DIFFERENT TIME SCALES

Time scale	Transfer function	Train function	Best epoch	Average absolute error	Average relative error
S1	tansig	trainlm	11	5.8683	9.07%
S2	tansig	trainlm	4	2.7563	4.23%
S3	tansig	trainlm	107	0.2259	0.35%
S4	tansig	trainlm	4	0.1131	0.17%
S5	tansig	trainlm	7	0.0651	0.10%

TABLE I reveals that, as the time scale increased from S1 to S5, the estimated error decreases. The average absolute error and relative error for the simulation of AR at time scale of S1 are $5.8683\times10^{8}m^{3}$ and 9.07% respectively, but those at time scale of S5 only are $0.0651\times10^{8}m^{3}$ and 0.10% respectively.

Figure 4 reveals the original data of AR and the simulated values by BPANN at different time scales respectively.

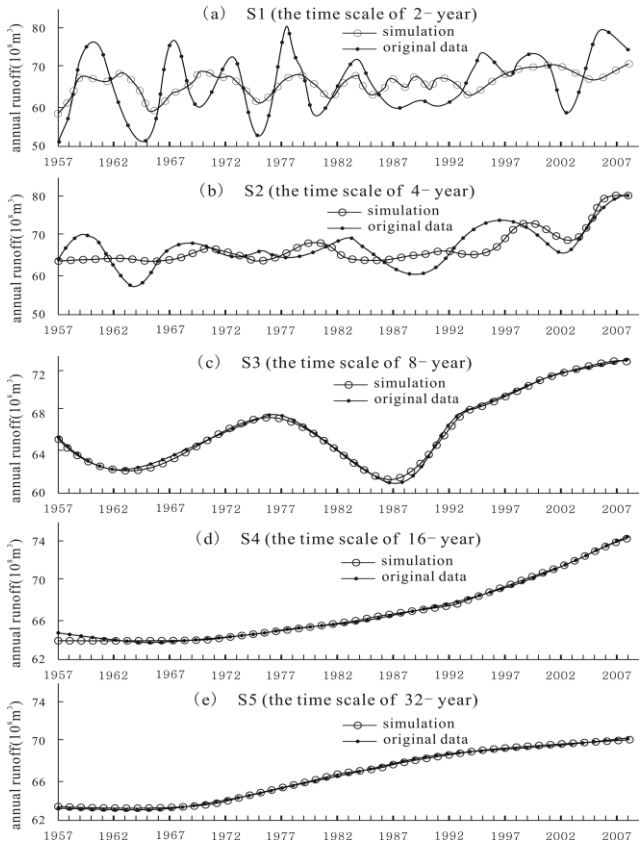

Figure 4. The Original Data of AR and Its Simulated Values by BPANN at Different Time Scales

To compare the simulated results by BPANN with those by multiple linear regression (MLR) at different time scales, we also employed the wavelet regression analysis, i.e. regression analysis based on the results of wavelet decomposition [18-19]. We used the method to fit a group of multiple linear regression equations (MLREs) between AR with AAT and AP at different time scales as shown in TABLE II.

TABLE II revealed that all MLREs at each time scale got across the statistical test at the significant level of 0.01 or 0.001, but the simulated error of each MLRE at the chosen time scales is different. The simulated errors of MLREs at the time scale of S1 and S2 (i.e. 2-year and 4-year scale) are relative large, that at the time scale of S3 (i.e. 8-year scale) are fairish, and the simulated errors of MLR at the time scale of S4 and S5 (i.e. 16-year and 32-year scale) appear small.

TABLE II. MLREs FOR THE RELATIONSHIP BETWEEN AR AND AAT & AP AT DIFFERENT TIME SCALES

Time scale	Regression equation	Significance level	Average absolute error	Average relative error
S1	$AR = 3.243AAT + 54.89$	0.01	6.266	9.665%
S2	$AR = 2.883AAT + 0.173AP + 43.62$	0.001	3.250	4.959%
S3	$AR = 5.792AAT + 0.116AP + 37.276$	0.001	0.880	1.354%
S4	$AR = 3.332AAT + 0.189AP + 40.618$	0.001	0.329	0.502%
S5	$AR = 2.555AAT + 0.206AP + 42.353$	0.001	0.109	0.165%

In order to test the simulation models, including the BPANN models and MLREs based on WD at different time scales, we computed the coefficient of determination as well as the AIC value as shown in Table III.

TABLE III. COMPARISON FOR BPANN MODELS AND MLREs AT DIFFERENT TIME SCALES

Time scale		S1	S2	S3	S4	S5
BPANN	CD	0.715	0.856	0.920	0.998	0.999
	AIC	118.49	72.51	22.28	-151.49	-259.21
MLRE	CD	0.087	0.362	0.894	0.975	0.996
	AIC	209.92	143.26	12.96	-96.71	-209.17

A higher coefficient of determination (CD) and a lower AIC value indicate a better model. TABLE III indicates that both of BPANN and MLRE is the best at time scale of S5 (i.e. 32-year scale), and the worst at the time scale of S1 (i.e. 2-year scale).

By comparing the two modeling methods above, i.e. the multiple linear regression (MLR) and back-propagation artificial neural network (BPANN) based on wavelet decomposition, we also conclude that the BPANN is better than the MLR at each time scale. In other words, both MLR and BPANN successfully simulated the hydro-climatic process based on wavelet analysis, but the effect from BPANN is better than that from the MLR.

IV. CONCLUSIONS

Taking the Yarkand River as an example, this study applied an integrated approach combining wavelet decomposition (WD), multiple linear regression (MLR), and back propagation artificial neural network (BPANN) to simulate the variation of streamflow and its response to the regional climate change at different time scales.

Our study also revealed that the hydro-climatic process at a large time scale (e.g. 16-year or 32-year scale) is basically a linear process, but at a small time scale (e.g. 2-year or 4-year scale) it is essentially a nonlinear process with complicated causations. Therefore, the estimated precision is high at a large time scale (e.g. 16-year or 32-year scale) because the time series of runoff are monotonically related to long-term climatic changes. However, it is difficult to accurately predict a nonlinear hydro-climatic process at a small time scale (e.g. 2-year or 4-year scale).

Nevertheless, the integrated approach combining wavelet decomposition (WD), multiple linear regression (MLR), and back propagation artificial neural network (BPANN) provides a way to understand the hydro-climatic process of Yarkand River from a multi-scale perspective. The approach can be used to explore the relationship between streamflow and its related climatic factors of other inland rivers in northwest China.

The main conclusions of this work can be summarized as follows:

(1)The integrated approach combining wavelet decomposition and BPANN successfully modeled the streamflow with climatic factors at different time scales. Moreover, the simulated effect at a larger time scale is better than that at a smaller time scale.

(2) The variation of runoff was a response to the regional climate change. In the past five decades, the annual runoff (AR) was mainly affected by annual average temperature (AAT) and annual precipitation (AP).

(3) Overall, the relationship between the AR with AAT and AP was successfully simulated by the multiple linear regression (MLR) as well as the back propagation artificial neural network (BPANN) based on wavelet decomposition (WD), but the simulated effect from BPANN based on WD is better than that from MLR based on WD.

(4) The variation patterns of temperature and precipitation were scale-dependent in time. Different time scales resulted in the different patterns of AAT and AP. At the time scale of S5, i.e. 32-year scale, AR presented a monotonically increasing trend with AAT and AP. But at the time scale of S1, S2, S3 and S4, i.e. 2-year, 4-year, 8-year and 16-year scale, AR presented nonlinear variation with fluctuations of AAT and AP.

REFERENCES

[1] A. J. Cannon, and I. G. McKendry, "A graphical sensitivity analysis for statistical climate models: Application to Indian monsoon rainfall prediction by artificial neural networks and multiple linear regression models", International Journal of Climatology, Wiley, 2002, vol. 22, pp. 1687–1708.

[2] J. H. Xu, Y. N. Chen, W. H. Li, M. H. Ji, S. Dong, "The complex nonlinear systems with fractal as well as chaotic dynamics of annual runoff processes in the three headwaters of the Tarim River", Journal of Geographical Sciences, Springer, 2009, vol. 19, no. 1, pp. 25–35.

[3] J. H. Xu, W. H. Li, M. H. Ji, F. Lu, S. Dong, "A comprehensive approach to characterization of the nonlinearity of runoff in the headwaters of the Tarim River, western China", Hydrological Processes, Wiley, 2010, vol. 24, no. 2, pp. 136–146.

[4] J. H. Xu, Y. N. Chen, F. Lu, W. H. Li, L. J. Zhang, Y. L. Hong, "The nonlinear trend of runoff and its response to climate change in the Aksu River, western China", International Journal of Climatology, Wiley, 2011, vol. 31, no. 5, pp. 687–695.

[5] J. H. Xu, Y. N. Chen, W. H. Li, Y. Yang, Y. L. Hong, "An integrated statistical approach to identify the nonlinear trend of runoff in the Hotan River and its relation with climatic factors", Stochastic Environmental Research and Risk Assessment, Springer, 2011, vol. 25, no. 2, pp. 223–233.

[6] J. H. Xu, Y. N. Chen, W. H. Li, Q. Nie, Y. L. Hong, Y. Yang, "The nonlinear hydro-climatic process in the Yarkand River, northwestern China", Stochastic Environmental Research and Risk Assessment, Springer, 2012, DOI: 10.1007/s00477-012-0606-9.

[7] J. H. Xu, Y. N. Chen, W. H. Li, S. Dong, "Long-term Trend and Fractal of Annual Runoff Process in Mainstream of Tarim River", Chinese Geographical Science, Springer, 2008, vol. 18, no. 1, pp. 77–84.

[8] M. Sabit, and A. Tohti, "An analysis of water resources and it's hydrological characteristic of Yarkend River Valley", Journal of Xinjiang Normal University (Natural Sciences Edition), vol. 24, no. 1, 74–78, 2005. (in Chinese)

[9] J. H. Xu, Y. N. Chen, W. H. Li, M. H. Ji, S. Dong, Y. L. Hong, "Wavelet Analysis and Nonparametric Test for Climate Change in Tarim River Basin of Xinjiang during 1959-2006", Chinese Geographical Science, Springer, 2009, vol. 19, no. 4, pp.306–313.

[10] D. Labat D, "Recent advances in wavelet analyses: Part 1. A review of concepts", Journal of Hydrology, Elsevier, 2005, vol. 314, pp. 275–288.

[11] S. G. Mallat, "A theory for multiresolution signal decomposition: the wavelet representation", IEEE Transactions Pattern Analysis and Machine Intelligence, IEEE, 1989, vol. 11, no. 7, pp. 674–693.

[12] L. M. Bruce, C. H. Koger, J. Li , "Dimensionality reduction of hyperspectral data using discrete wavelet transform feature extraction", IEEE Transactions on Geoscience and Remote Sensing, IEEE, 2002, vol. 40, no. 10, pp. 2331–2338.

[13] K. Hsu, H. V. Gupta, S. Sorooshian, "Artificial neural network modeling of the rainfall-runoff process", Water resources research, AGU, 1995, vol. 31, no. 10, pp. 2517–2530.

[14] H. R. Maier, and G. C. Dandy, "The effect of internal parameters and geometry on the performance of back-propagation neural networks: an empirical study", Environmental Modelling & Software, Elsevier, 1998, vol. 13, pp. 193-209.

[15] J. H. Xu, "Mathematical methods in contemporary geography", Higher Education Press, Beijing, 2002, pp. 37–105.

[16] D. R. Anderson, K. P. Burnham, W. L. Thompson, "Null hypothesis testing: problems, prevalence, and an alternative", Journal of Wildlife Management, Wiley, 2000, vol. 64, no. 4, pp. 912–923.

[17] Y. N. Chen, K. Takeuchi , C. C. Xu, Y. P. Chen, Z. X. Xu, "Regional climate change and its effects on river runoff in the Tarim Basin, China", Hydrological Processes, Wiley, 2006, vol. 20, pp. 2207–2216.

[18] J. H. Xu, Y. N. Chen, M. H. Ji, F. Lu, "Climate change and its effects on runoff of Kaidu River, Xinjiang, China: A multiple time-scale analysis", Springer, Chinese Geographical Science, Springer, 2008, vol. 18, no. 4, pp. 331–339.

[19] J. H. Xu, Y. W. Xu, C. N. Song, "An Integrative Approach to Understand the Climatic-Hydrological Process: A Case Study of Yarkand River, Northwest China," Advances in Meteorology, Hindawi Publishing Corporation, 2013, vol. 2013, Article ID 272715, 9 pages. doi:10.1155/2013/272715.

[20] B. G. Sun, W. Y. Mao, Y. R. Feng, T. Chang, L. P. Zhang, and L. Zhao, "Study on the Change of Air Temperature, Precipitation and Runoff Volume in the Yarkant River Basin", Arid Zone Research, vol. 23, no. 2, pp. 203–209, 2006. (in Chinese).

[21] J. H. Xu, Y. N. Chen, W. H. Li, P. Y. Peng, Y. Yang, C. N. Song, C. M. Wei, and Y. L. Hong, "Combining BPANN and Wavelet Analysis to Simulate Hydro-climatic Processes--A Case Study of the Kaidu River, NW China", Frontiers of Earth Science, vol. 7, no. 2, pp. 227-237.

[22] J. H. Xu, Y. N. Chen, W. Li, S. Dong, "Signal processing for the annual runoff process by wavelet and R/S analysis: A case study of the Tarim headwater basin", In Signal Processing, 2008. ICSP 2008. 9th International Conference on. IEEE, pp. 2746-2749.